# Drop-by-drop radar cross section calculations for Sand C-band weather radar frequencies

Franz Teschl<sup>1\*</sup>, Merhala Thurai<sup>2</sup>, Sophie Steger<sup>1</sup>, Michael Schönhuber<sup>3</sup>

\* franz.teschl@tugraz.at

<sup>1</sup> Graz University of Technology, 8010 Graz, Austria

<sup>2</sup> Department of Electrical and Computer Engineering, Colorado State University, Fort Collins, CO 80523, USA

<sup>3</sup> JOANNEUM RESEARCH Forschungsgesellschaft mbH, 8010 Graz, Austria

Abstract— Recent studies revealed that scattering calculations at weather radar frequencies using individual drop shapes result in better agreement between simulated and measured polarimetric weather radar parameters, than if established rotational symmetric shape models are used. In the present work, thousands of individual rain drops that were detected with a 2D Video Disdrometer during a tropical storm, were reconstructed and their individual radar cross sections (RCS) were calculated by automatizing a commercial EM solver software. The calculations were carried out at the common weather radar frequencies at 2.8 GHz and 5.625 GHz, both for horizontal and vertical polarization. It is evaluated to what extend the RCS can differ for drops with an equal volume, it is discussed how the scattering parameters of individual drops scale within S- and C-band frequencies, and it is shown for one sample drop what effect the modelling granularity has on determined radar cross section values.

*Index Terms*— scattering calculation, hydrometeors, rain drop shapes, radar cross section, RCS, 2D Video Disdrometer, S-band, C-band.

### I. INTRODUCTION

As rain drops interact with microwaves, their actual shapes and their distribution within a certain volume are crucial for modelling wave propagation through the troposphere. Scattering calculations are of interest for applications in radiocommunications and in remote sensing, e.g. for satellite communications [1] and weather radar meteorology [2].

For a long time, in these disciplines, raindrops were primarily modelled as rotationally symmetric ellipsoids since for such ellipsoids, as for spheres, an exact solution for the wave scattering problem exits. Some of the well-known methods for scattering from oblate raindrops are (i) point-matching method [3], (ii) Fredholm Integral-equation Method [4], and T-matrix method [5]. Although these assume that drops have rotational axis of symmetry, they can take into account non-zero canting angles. In turbulent weather situations, however, a significant number of drops exhibit no rotational symmetry, e.g. due to turbulence, drop collisions and the asymmetric drop oscillation modes induced as a result. Scattering calculations for asymmetric drops can markedly differ from those of oblate spheroids, as e.g. presented in [6].

In previous studies it could be shown that scattering calculations using individual drop shapes resulted in better agreement between simulated and measured polarimetric weather radar parameters, than if established rotational symmetric shape models are used. Such studies have been carried out for C- and S-band frequencies, [7] and [8]. In those studies, rain drops detected with imaging disdrometers were reconstructed and their individual radar cross sections were calculated with a commercial EM solver software. These scattering calculations are very time consuming, especially when the individual drops are modeled by a fine triangular mesh.

The present paper investigates what effect reducing the modelling granularity, that causes time consuming computations, has on determined radar cross section values of an asymmetric raindrop. Furthermore, it is evaluated whether or not the RCS of a drop can be estimated with high precision, if the RCS for another frequency within the C- or S-band is known.

# II. RAIN EVENT AND OBSERVATIONS

The rain event considered for this study occurred on July 12, 2020, at the University of Alabama in Huntsville (UAH), USA. At this site, among other meteorological sensors, two 2D Video Disdrometers (2DVD) are installed. These specialized disdrometers provide front and side view information as well as falling velocity of individual precipitation drops. The two instruments are co-located; while one instrument is installed within a double wind fence, the other is installed outside the fence [9].

The rain even lasted approx. for three hours from ~15:00 UTC until 18:00 UTC. During the observing period, thousands of individual drops were detected. All drops with an equal volume diameter > 2 mm were reconstructed in 3D using the raw-data from the 2DVDs. With the instrument that was protected by the double wind fence wind, 10544 drops > 2 mm have been detected during the rain event, while 8048 drops were detected with the 2DVD outside of the wind fence. The plots of velocity vs. diameter are shown in Fig 1(a) and Fig 1(b). A research-grade 3D-sonic anemometer was used to characterize the turbulent flow and was sited 3 m upwind from the wind fence (see [10]).

The histograms of fall speeds for  $3\pm0.1$  mm drops from these two instruments during turbulent period are shown in Fig. 2. The histogram shapes are similar to each other, implying that the wind-fence-induced effects did not change the environmental turbulent flow at the sensing area. Note also in [10], a noticeable reduction in fall velocities was observed during the turbulent period.

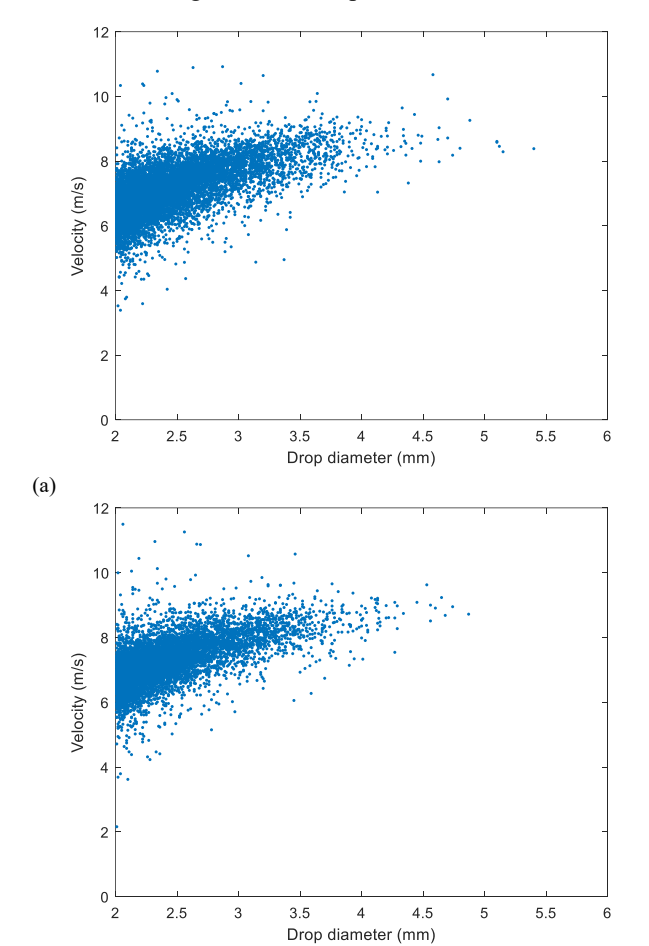


Fig. 1. Velocity vs. diameter for drops > 2mm detected with 2DVDs, protected by a double wind fence (a) and outside the wind fence (b).

(b)

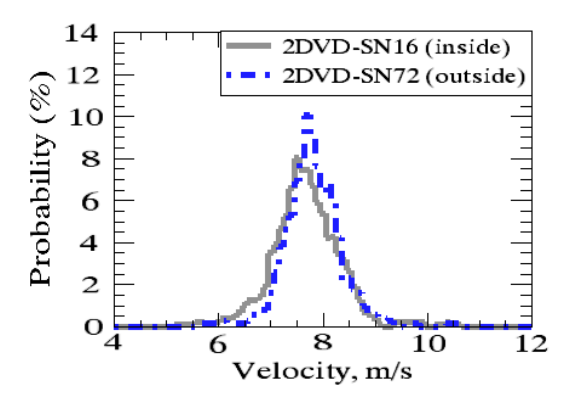


Fig. 2. Histograms of fall speeds for 2.9 to 3.1 mm drops from 2DVD measurements inside (SN16) the double wind fence and the one located outside the fence (SN72). Time period of turbulance is 15:12 to 15:36 UTC (12 July 2020, UAH).

## III. SCATTERING CALCULATIONS

In order to determine the radar cross section (RCS), scattering calculations have been carried out for all of the 18592 rain drops > 2 mm. The simulation program used within this study is Microwave Studio of the CST Studio Suite 2020. In particular, the build in integral equation solver was used. In order to automatize the calculation for the huge amount of drops, the CST Microwave Studio was controlled by using a Visual Basic for Applications (VBA) script. This concept was already used in previous studies [8] and is described in more detail in [7].

In the present study, the RCS of individual drops has been determined for two common S- and C- band weather radar frequencies: 2.8 GHz and 5.625 GHz. From the raw data of the two 2DVD, the three dimensional shape of each drop was reconstructed. The 3D reconstruction procedure is described in [11, 12]. Figure 3 shows front and side view of the biggest drop that was detected after 3D reconstruction. In order that the shape information can be imported into Microwave Studio, the 3D information was converted to an STL-file that characterizes the surface geometry of the drop without specifying the material information.

For the material the dielectric properties of water were assumed, by applying the formulae by Ray [13]. This model provides the complex permittivity values for water and ice as a function of the frequency and the temperature. Assuming a temperature of  $22^{\circ}$  C the complex permittivity  $\epsilon$  for water is

$$\epsilon = 72.5 - j22.43$$
 for 5.625 GHz  $\epsilon = 77.7 - j11.66$  for 2.8 GHz

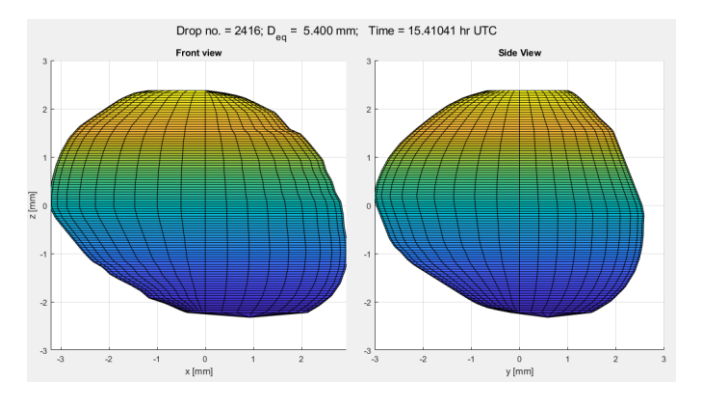


Fig. 3. Front and side view of the biggest drop that was detected with one of the two 2D Video Disdrometers during the rain event (drop no. 2416). The equal volume diameter is 5.4 mm.

# IV. SIMULATION RESULTS

Figure 4 shows the calculated radar cross sections for all of the detected rain drops with a diameter > 2 mm at 2.8 GHz frequency. The respective results for the RCS at 5.625 GHz are shown in Fig. 5.

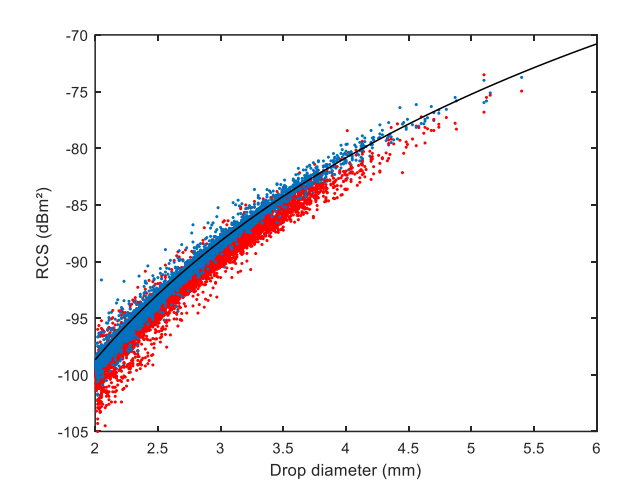


Fig. 4. RCS of 18592 individual rain drops for horizontal (in blue) and vertical polarization (in red) at 2.8 GHz S-Band frequency. The solid line represents the Mie-Solution of the RCS of a sphere with the indicated diameter.

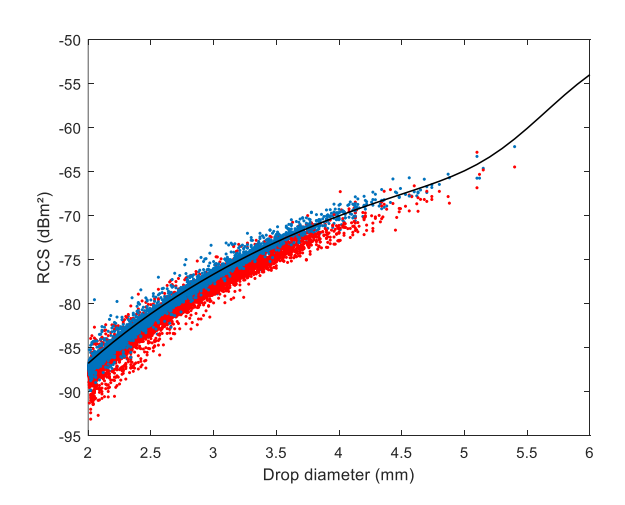


Fig. 5. RCS of 18592 individual rain drops for horizontal (in blue) and vertical polarization (in red) at 5.625 GHz C-Band frequency. The solid line represents the Mie-Solution of the RCS of a sphere with the indicated diameter.

When the RCS at 5.625 GHz of each individual drop is plotted against its RCS at 2.8 GHz, it results in an apparently linear relationship (Fig 6). This is true for both, horizontal and vertical polarization. In fact, for drops from 2 mm up to 5 mm in diameter, the RCS at 5.625 GHz is between 10 dB and 12 dB higher than the RCS at 2.8 GHz. Fig. 7 shows this difference for horizontal and vertical polarization as a function of the drop diameter. The plotted solid line in the figure is not a regression, but it illustrates the difference between the RCS at the mentioned frequencies for spherical water drops, according to Mie-Theory [14]. As the curves for the sphere is in accordance with the results of the thousands of drops for which scattering was determined individually, it seems that the RCS can be estimated for a given frequency within S- and C-band, if the result at another frequency within this range has already been determined. For drop sizes

up to 4 mm, this estimation is within 0.5 dB. As the computation time of the RCS of individual drops can be considerable, such an estimation may be useful e.g. when comparing simulations and weather radar measurements. In this present study, only some hundred drops were detected with a diameter > 4 mm. However, the results in Fig. 7 indicate that for these bigger drops the ratio between the RCS at 2.8 GHz and 5.625 GHz is not so predictable, if the result at one of these frequencies is known.

## V. ACCURACY CONSIDERATIONS

Fig. 8 shows exemplary the RCS for both horizontal and vertical polarization at 5.625 GHz frequency for drop no. 2416 (pictured in Fig. 9) as a function of the view angle. The RCS results are shown for different degrees of modelling accuracy of the drop shape.

It can be noticed that the RCS for horizontal polarization is always higher than that for vertical polarization, which is explained by the oblate shape of that drop in question. It is also noticeable that the RCS depends stronger on the view angle for horizontal polarization that for vertical polarization, which is due to the absence of rotational symmetry of the drop.

In Fig. 8 the RCS of the drop is shown for various triangle mesh settings: The highest values for the RCS result in a representation of the drop by 1840 triangular surfaces as shown in Fig 9 (a). Applying such a fine mesh, the drop model features a surface area of 92.5 mm<sup>2</sup>. It is also shown in the figure, that coarser triangle mesh settings result in a lower reported RCS value at all view angles.

It was also investigated what maximal numbers triangular surfaces are practicable. When modelling the drop with 7600 surfaces, which means that each of the surfaces in Fig 9 (a) is again divided into four parts, the computation time is typically more than 10 minutes and in this very case of drop no. 2416, the simulation in the end did not terminate. Applying a mesh with 7600 triangular surfaces would lead to a surface area of 93.9 mm<sup>2</sup>.

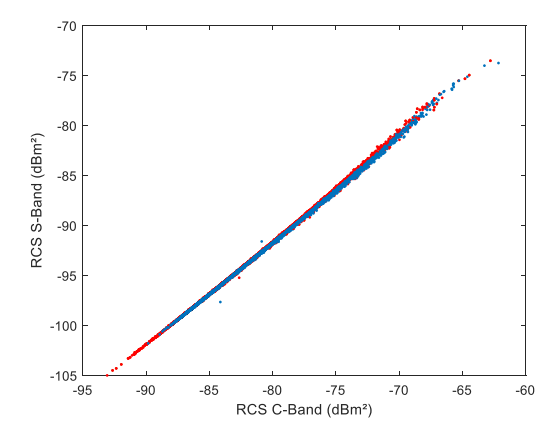
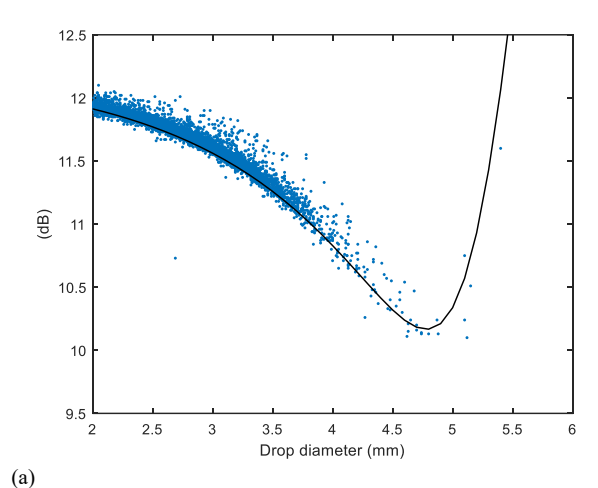


Fig. 6. RCS at 5.625 GHz vs. RCS at 2.8 GHz for each of the 18592 individual drops; horizontal polarization in blue and vertical polarization in red.



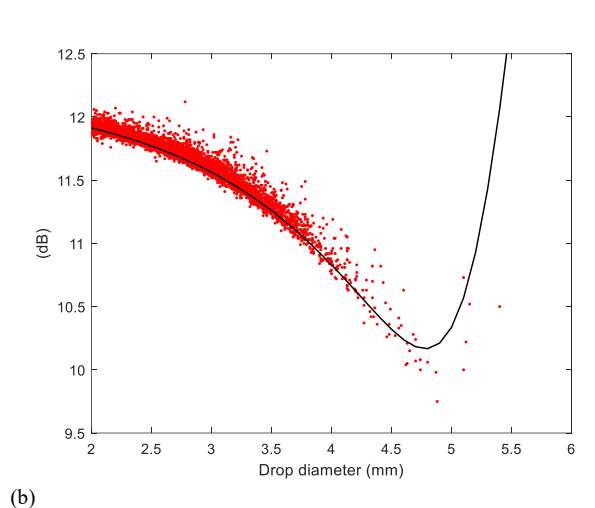


Fig. 7. Ratio in dB by which the horizontal RCS of each of the investigated 18592 drops is higher at 5.625 GHz than at 2.8 GHz for horizontal polarization (a) and vertical polarization (b). The solid line represents the respective ratio at the mentioned frequencies for spherical water drops, according to Mie-Theory.

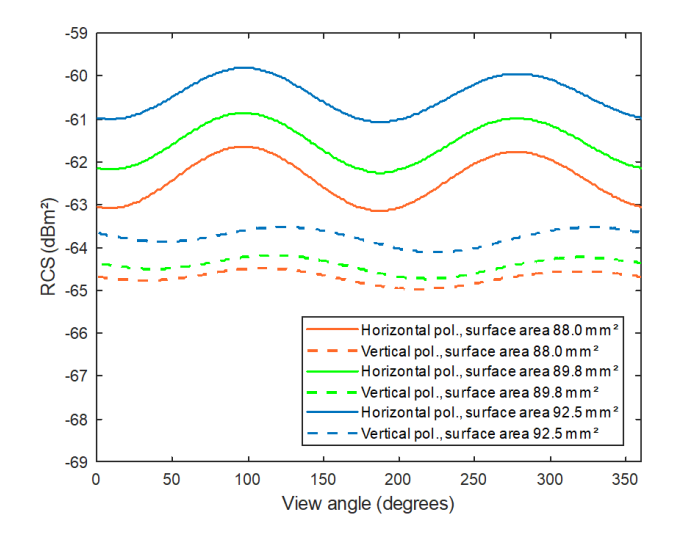
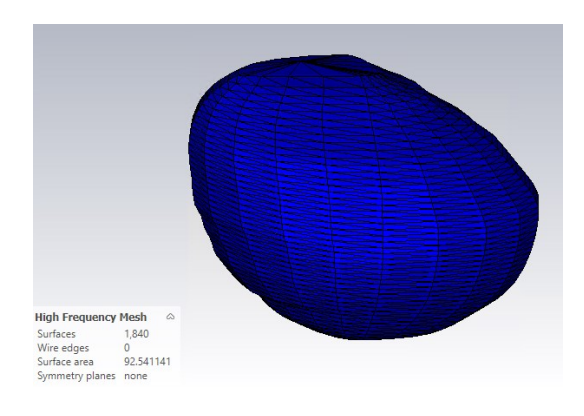


Fig. 8. RCS for horizontal and vertical polarization at 5.625 GHz C-Band frequency for drop no. 2416 as a function of the view angle. The RCS results are shown for different degrees of modelling accuracay of the drop shape.



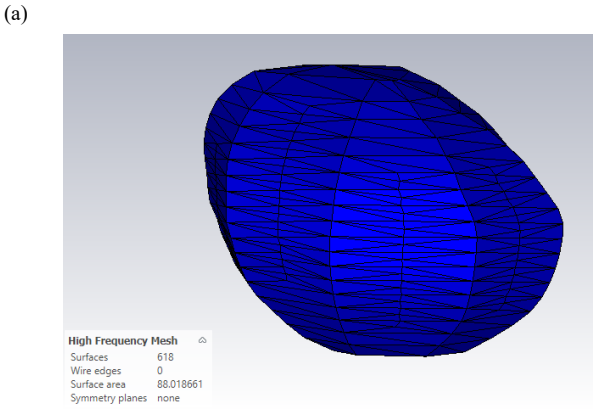


Fig. 9. Triangulation of drop no. 2416, with 1840 triangular surfaces and a total surface area of  $92.5~\text{mm}^2$  (a) and with 618~surfaces, leading to a total surface area of  $88~\text{mm}^2$  (b).

## VI. SUMMARY AND CONCLUSIONS

Thousands of individual rain drops that were detected with a 2D Video Disdrometer during a tropical storm, were reconstructed and their individual RCSs were calculated with a commercial EM solver software (CST Studio Suite 2020 with integral equation solver). The calculations were carried out at the common weather radar frequencies at 2.8 GHz and 5.625 GHz, both for horizontal and vertical polarization.

Following conclusions can be drawn:

(b)

- The simulations showed that the individual RCSs can differ by ~6 dB from that of equal volume water spheres.
- If the RCS for either C- or S-band is known, the RCS for the respective other band can be estimated with a very high probability. This is true both for horizontal and for vertical polarization.
- For drop sizes up to 4 mm this estimation is within 0.5 dB.
- For drops > 4 mm the relationship between the RCS at Cor S-band of any drop seems to follow that of an equal volume sphere, however, only some hundred drops > 4 mm were detected within the observed rain event.

When it comes to the drop-by-drop scattering calculation it has to be mentioned, that a triangulation of one drop by up to 2000 triangular surfaces can be handled within a few minutes with powerful contemporary personal computers. It has been noticed that a triangulation with > 5000 surfaces would lead to computation times of 10 minutes and more and also increases the risk that the resulting equation system cannot be solved.

A triangulation that best represents the actual surface area of the drop will – in general – also lead to an ideal representation of its volume. The study has also shown that not necessarily the number of triangles is crucial for the accuracy of the simulation, but how good the surface and the volume are represented by the triangulation.

Finally, as has been shown in some of our past studies, 'drop-by-drop' scattering calculations [6-8] are important for understanding of the role of drop shapes in the overall retrieval (or estimation) of rainfall rates from polarimetric radar data. Another equally important factor is the fall velocities of drops especially during turbulent conditions. The joint effect (due to shape variations and fall velocity variations) will be considered in the near future.

### REFERENCES

- [1] A. Paraboni, A. Martellucci, C. Capsoni, and C.G. Riva: "The physical basis of atmospheric depolarization in slant paths in the V band: theory, Italsat experiment and models," IEEE transactions on antennas and propagation 59 (11), 4301-4314.
- [2] T. A. Seliga, and V. N. Bringi, 1978: "Differential reflectivity and differential phase shift: Applications in radar meteorology," Radio Sci., 13, 271–275, https://doi.org/10.1029/RS013i002p00271.
- [3] T. Oguchi, "Electromagnetic wave propagation and scattering in rain and other hydrometeors," in Proceedings of the IEEE, vol. 71, no. 9, pp. 1029-1078, Sept. 1983, doi: 10.1109/PROC.1983.12724.
- [4] N. K. Uzunoglu, B. G. Evans, and A. R. Holt: "The scattering of electromagnetic radiation by precipitation particles and propagation characteristics of terrestrial and space communication systems". IEE Proc, 124, 417–424, 1997.
- [5] M. I. Mishchenko, L. D. Travis, and D. W. Mackowski: "T-matrix computations of light scattering by nonspherical particles: A review". J. Quant. Spectrosc. Radiat. Transfer, 55, 535–575, 1996, doi:10.1016/0022-4073(96)00002-7.
- [6] M. Thurai, S. Manić, M. Schönhuber, V. N. Bringi, and B. M. Notaroš, "Scattering calculations at C-Band for asymmetric raindrops reconstructed from 2D video disdrometer measurements", J. Atmos. Oceanic Technol., vol. 34, pp. 765–776, 2017. https://doi.org/10.1175/JTECH-D-16-0141.1.
- [7] M. Thurai, S. Steger, F. Teschl, and M. Schönhuber. "Analysis of Raindrop Shapes and Scattering Calculations: The Outer Rain Bands of Tropical Depression Nate". *Atmosphere*. 2020; 11(1):114. https://doi.org/10.3390/atmos11010114
- [8] M. Thurai, S. Steger, F. Teschl, M. Schönhuber and D.B. Wolff, "Rain Drop Shapes and Scattering Calculations: A Case Study using 2D Video Disdrometer Measurements and Polarimetric Radar Observations at S-band During Hurricane Dorian Rain-Bands," 15th European Conference on Antennas and Propagation (EuCAP), Virtual Conference, March 2021, doi: 10.23919/EuCAP51087.2021.9411181.
- [9] M. Thurai, V. Bringi, P.N. Gatlin, W.A. Petersen, and M.T. Wingo, "Measurements and Modeling of the Full Rain Drop Size Distribution," Atmosphere 2019, 10, 39, https://doi.org/10.3390/atmos10010039.

- [10] M. Thurai, V. Bringi, P. Gatlin, and M. Wingo, "Raindrop fall velocity in turbulent flow: an observational study," Adv. Sci. Res., 18, 33–39, 2021, https://doi.org/10.5194/asr-18-33-2021.
- [11] M. Schönhuber, M. Schwinzerl and G. Lammer, "3D Reconstruction of 2DVD-measured raindrops for precise prediction of propagation parameters," 2016 10th European Conference on Antennas and Propagation (EuCAP), Davos, Switzerland, 2016, pp. 1-4, doi: 10.1109/EuCAP.2016.7481929.
- [12] M. Schwinzerl, M. Schönhuber, G. Lammer, and M. Thurai, "3D reconstruction of individual raindrops from precise ground-based precipitation measurements," EMS Annu. Meet. Abstr. 2016, 13, EMS2016-601, Trieste, Italy, September, 2016.
- [13] P. Ray, "Broadband complex refractive indices of ice and water," Appl. Opt. 1972, vol. 11, pp. 1836–1844.
- [14] G. Mie, Beiträge zur Optik trüber Medien, speziell kolloidaler Metallösungen, Annalen der Physik, 1908, (4) 25, 377-445.